Actas Dermo-Sifiliográficas 117 (2026) 104714

Contents lists available at ScienceDirect

Actas Dermo-Sifiliográficas

journal homepage: www.actasdermo.org

Original Article

# Perfusion Analysis by Laser Speckle Predicts the Extent of Skin Graft Necrosis

A. Pinho [a,b,*], A. Brinca [a,b], R. Vieira [a,b]

[a] Serviço de Dermatologia, Hospitais da Universidade de Coimbra, Unidade Local de Saúde de Coimbra, Praceta Prof. Mota Pinto, 3000-075 Coimbra, Portugal
[b] Faculdade de Medicina, Universidade de Coimbra, Azinhaga de Santa Comba, 3000-548 Coimbra, Portugal

ARTICLE INFO

*Keywords:*
Laser speckle contrast imaging
Postoperative complications
Skin transplantation
Time factors
Graft survival

ABSTRACT

*Background and aims:* Skin graft necrosis is a common complication in dermatologic surgery, but reliable methods for predicting its occurrence are lacking. Laser speckle contrast imaging (LSCI) is a validated tool for studying skin graft microcirculation. We aimed to analyze the relationship between perfusion, assessed intraoperatively or postoperatively with LSCI, and the extent of necrosis on day 28. In addition, we aimed to determine whether perfusion can predict the development of clinically significant necrosis, defined as necrosis affecting 20% or more of the graft.

*Materials and methods:* Fifty-five adults undergoing skin grafting after skin cancer excision were included. Perfusion was assessed with LSCI intraoperatively on the wound bed and on the graft surface on day 7. The extent of necrosis was determined on day 28.

*Results:* Graft necrosis was significantly correlated with graft bed perfusion assessed on day 0 ($r = -0.86$) and graft perfusion assessed on day 7 ($r = -0.69$). Significant linear regression models showed that intraoperative graft bed perfusion and day 7 graft perfusion explained 75% and 46% of the variability in necrosis extent, respectively. Overall, each unit increase in graft bed perfusion reduced necrosis extent by 41 percentage points, whereas each unit increase in day 7 graft perfusion reduced necrosis extent by 21 percentage points. The perfusion threshold with the highest predictive value for clinically significant necrosis was identified in the graft bed.

*Conclusions:* LSCI may provide valuable information as a predictive tool for necrosis through rapid, noninvasive perfusion analysis, allowing the identification of patients who are optimal candidates for skin grafting and those who may require prolonged wound care.

## Introduction

Skin graft necrosis is a common complication in skin cancer reconstructive surgery and may take several weeks to become established, leading to longer healing times, increased morbidity, and higher health care costs.[1,2] This complication arises from the nature of a skin graft, which involves the transfer of free cutaneous tissue from a donor site to a recipient site after intentional separation.[3] Direct anastomoses between the graft and recipient bed vessels, known as inosculation; ingrowth of recipient bed vessels toward the graft, known as angiogenesis; development of new blood vessels from undifferentiated bone marrow stem cells, known as vasculogenesis; and controlled regression and replacement of the native vascular network are critical steps in skin graft reperfusion.[4,5] Disruption of any of these processes is expected to result in graft hypoperfusion and necrosis.

It is empirically accepted that higher graft bed perfusion is associated with a lower risk of graft necrosis.[1] Nevertheless, no reliable clinical features of the graft bed or graft surface can predict the occurrence of late necrosis.

During the last decade, LSCI has shown promise for evaluating cutaneous microcirculation in various medical and surgical fields, such as dermatology, rheumatology, ophthalmology, and surgery.[6–8] This noninvasive, fast, and easily operated imaging technique can provide valuable information on the perfusion of skin flaps and grafts.[9–11] The underlying principle is that when the skin is illuminated with coherent light, such as a laser in the near-infrared spectrum, for example, 780 nm, an interference pattern of backscattered light, displayed as a granular pattern of dark and bright spots, can be identified with a detector. This is known as the speckle pattern. LSCI is based on dynamic changes in this

*Abbreviations:* APU, arbitrary perfusion units; CI, confidence interval; CVC, cutaneous vascular conductance; LSCI, laser speckle contrast imaging; MAP, mean arterial pressure.

* Corresponding author.
*E-mail address:* 10648@ulscoimbra.min-saude.pt (A. Pinho).

https://doi.org/10.1016/j.ad.2026.104714
Received 29 November 2024; Accepted 28 January 2025
Available online 24 June 2026
0001-7310/© 2026 Published by Elsevier España, S.L.U. on behalf of AEDV. This is an open access article under the CC BY-NC-ND license (http://creativecommons.org/licenses/by-nc-nd/4.0/).

speckle pattern caused by the interaction of coherent light with moving red blood cells.[12,13] The penetration depth of LSCI is approximately 300 μm. Therefore, it mainly records blood flow in the superficial papillary plexus, which forms part of the cutaneous microcirculation.[14]

If perfusion assessed by LSCI, either on the graft bed or on the graft surface, is closely linked to the extent of skin graft necrosis, this technique may help select the best candidates for immediate graft closure and identify patients at risk of necrotic complications and prolonged wound care.

We aimed to analyze the relationship between perfusion, assessed intraoperatively or postoperatively with LSCI, and the extent of necrosis on day 28, and to propose predictive models for graft necrosis based on perfusion. In addition, we aimed to determine whether perfusion could serve as a predictive factor for the development of clinically significant necrosis.

## Materials and methods

### *Study design and population*

We designed a prospective longitudinal observational study with a 28-day follow-up period. The study followed the ethical standards outlined in the Declaration of Helsinki and was approved by the local ethics committee of our university hospital. Consecutive sampling was performed among adults eligible for skin cancer excision on the face, scalp, or limbs, followed by closure with a full-thickness or split-thickness skin graft at our dermatologic surgery unit.

The exclusion criteria were axillary temperature greater than 37.5 °C, inability to remain still during LSCI recording, grafts with donor or recipient sites involving the eyelids or nose, and postoperative bacterial graft infection or hematoma. These criteria were established to avoid measurement bias with LSCI, including bias caused by involuntary movement of underlying structures, such as the eyelids or nasal valve, and inability to assess the entire graft surface in a single recording, for example, in a pannasal graft.

The inclusion period was from April 2023 to January 2024. Anticipating a 10% dropout rate and accepting an $\alpha$ risk of 0.05 and a $\beta$ risk of 0.20 in a 2-sided test, the required sample size for detecting a correlation coefficient of 0.4 was 52 participants.

### *Outcome and factor*

The outcome was skin graft necrosis on day 28, defined as any loss of surface integrity, ranging from epidermolysis progressing to scab formation to full-thickness necrosis. Necrosis extent corresponded to the percentage of necrotic graft tissue. Clinically significant graft necrosis was defined as 20% or greater necrosis extent, as adopted by other study groups and implying the need for ongoing wound care.[15,16] The studied factor was perfusion assessed by LSCI on the graft bed on day 0 and on the graft surface on day 7.

### *Study procedures*

Participant characteristics included in the analysis, such as age, sex, history of arterial hypertension, dyslipidemia, or diabetes, current smoking, and use of anticoagulant or antiplatelet drugs, were collected during the preoperative evaluation. There were no changes to the reconstructive algorithms of our department or to standard postoperative wound care for this study.

Lesions were removed after infiltration with lidocaine 2% and epinephrine 1:100,000. The depth of dissection was the galea aponeurotica on the scalp, the superficial musculoaponeurotic system on the face, and the subcutaneous tissue or deep fascia on the limbs. Full-thickness skin grafts were harvested from the infraclavicular area for facial and scalp defects. Split-thickness skin grafts measuring 0.4 mm were harvested from the inner arm for upper limb defects and from the anterior thigh for lower limb defects. A tie-over dressing was applied for 1 week, and a new dressing with petrolatum gauze was used thereafter.

During surgery, graft bed perfusion, expressed in arbitrary perfusion units (APU), was assessed with the PeriCam PSI NR® LSCI system (Perimed, Järfälla, Sweden) at least 15 min after skin cancer removal. On day 7, at the first postoperative graft dressing change, graft perfusion was also evaluated. Each LSCI recording lasted 60 s and was performed at a distance of 25 cm from the skin. The studied area was immobilized with a vacuum pillow (AB Germa, Kristianstad, Sweden) to avoid movement artifacts.

To obtain a more physiological and comparable evaluation, perfusion in APU was divided by each participant's mean arterial pressure (MAP), yielding cutaneous vascular conductance (CVC).[14] CVC reflects the ease with which blood flows through the skin microcirculation at a given pressure difference.[17]

Skin graft evolution was recorded using sequential clinical photographs, which included a surgical ruler placed close to the graft. Necrosis extent was calculated from the clinical photographs obtained on day 28 by dividing the necrotic area by the total graft area. These areas were delimited and calculated with SketchAndCalc™ version 6.3.0 because the clinical photographs contained a surgical ruler that served as a scale. Fig. 1 presents examples of clinical photographs and LSCI recordings on days 0, 7, and 28 for grafts on the face and scalp.

### *Statistical analysis*

The sample underwent descriptive statistical analysis, and variable normality was assessed using the Shapiro–Wilk test. Correlation analysis was used to determine the relationship between perfusion and necrosis extent. Univariable linear regression was used to identify significant predictors of necrosis, and multivariable models incorporated statistically significant predictors.

Comparative analyses between groups, with and without necrosis extent of 20% or greater, were performed using the $\chi^2$ test, Fisher exact test, and Mann–Whitney $U$ test, as appropriate. A binary logistic regression model was used to estimate the odds ratio for necrosis extent of 20% or greater. Receiver operating characteristic curves were generated to predict necrosis extent of 20% or greater and to determine the perfusion cutoff points with the highest accuracy using the Youden index. Positive and negative predictive values were calculated.

All analyses were conducted using IBM SPSS Statistics, version 26. Statistical significance was set at $P < .05$.

## Results

A total of 55 participants completed the study, and 55 defects were reconstructed using 31 full-thickness and 24 split-thickness skin grafts. Table 1 summarizes patient, graft bed, and graft characteristics overall and according to categories of necrosis extent.

### *Correlation analysis between perfusion and necrosis*

Fig. 2 presents scatterplots showing the distribution of necrosis extent on day 28 and perfusion assessed on the graft bed and graft surface, revealing nonlinear negative relationships. A curve estimation approach showed that the logarithmic model provided the best fit for these relationships. Subsequently, the CVC variable underwent logarithmic transformation, allowing linearization of the correlations and linear regression analysis. The following perfusion results are presented as the natural logarithm of CVC [ln(CVC)].

Perfusion assessed on the graft bed was very strongly correlated with necrosis extent on day 28 ($r = -0.86$; $P < .001$). On day 7, the correlation between graft perfusion and necrosis extent was strong ($r = -0.69$; $P < .001$). These correlations differed significantly ($z = 2.2$; $P = .012$).

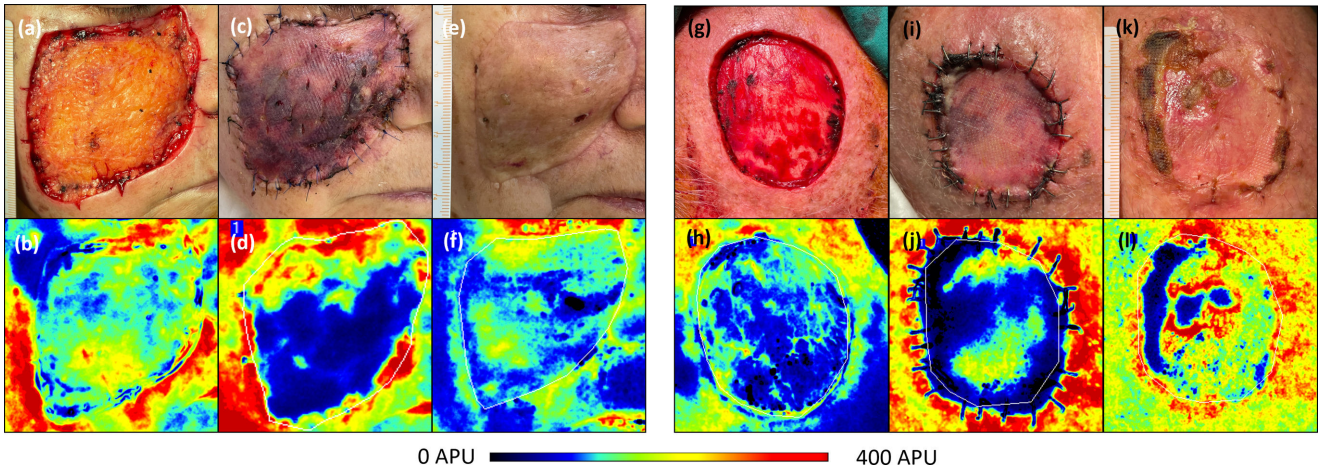


**Fig. 1.** Clinical photographs and LSCI recordings of full-thickness skin grafts. Clinical photographs (upper panels) and LSCI recordings (lower panels) of full-thickness skin grafts on the face, without clinically significant necrosis, and scalp, with clinically significant necrosis. Upper and lower panels refer to the same evaluation point: graft bed (A, B and G, H), graft on day 7 (C, D and I, J), and graft on day 28 (E, F and K, L). The LSCI software generates blood perfusion images of the scanned area using a semiquantitative color scale, ranging from black, indicating no perfusion, to red, indicating intense perfusion. Perfusion is also provided in arbitrary perfusion units (APU), not shown. Cutaneous vascular conductance is obtained by normalizing APU to the patient's mean arterial pressure.

**Table 1**
Patient, graft bed, and graft characteristics overall and according to the necrosis extension categories.

| Characteristics | Overall ($n$ = 55) | Necrosis <20% ($n$ = 37) | Necrosis ≥20% ($n$ = 18) | $P$ value |
|---|---|---|---|---|
| *Participant characteristics* | | | | |
| Age, median (range), y | 82.0 (61–96) | 83.3 (61–96) | 77.5 (68–90) | .09 |
| Female sex, No. (%) | 24 (43.6) | 14 (37.8) | 10 (55.6) | .21 |
| Current smoking, No. (%) | 2 (3.6) | 1 (2.7) | 1 (5.6) | .55 |
| Arterial hypertension, No. (%) | 45 (81.8) | 30 (81.1) | 15 (83.3) | .58 |
| Dyslipidemia, No. (%) | 34 (61.8) | 23 (62.2) | 11 (61.1) | .58 |
| Diabetes mellitus, No. (%) | 14 (25.5) | 12 (32.4) | 2 (11.1) | .08 |
| Antiplatelet therapy, No. (%) | 9 (16.4) | 6 (16.2) | 3 (16.7) | .62 |
| Anticoagulant therapy, No. (%) | 11 (20.0) | 8 (21.6) | 3 (16.7) | .48 |
| *Graft bed characteristics* | | | | |
| Location, No. (%) | | | | .01 |
| Face | 9 (16.4) | 8 (21.6) | 1 (5.6) | |
| Scalp | 22 (40.0) | 17 (45.9) | 5 (27.8) | |
| Upper limb | 4 (7.3) | 4 (10.8) | 0 (0.0) | |
| Lower limb | 20 (36.4) | 8 (21.6) | 12 (66.7) | |
| Type of graft, No. (%) | | | | .02 |
| Full-thickness | 31 (56.4) | 25 (67.6) | 6 (33.3) | |
| Split-thickness | 24 (43.6) | 12 (32.4) | 12 (66.7) | |
| Area, median (range), $cm^2$ | 14.1 (5.5–74.8) | 15.2 (5.8–74.8) | 13.0 (5.5–47.1) | .38 |
| CVC graft bed, mean (SD), APU/mm Hg | 0.86 (0.37) | 1.06 (0.28) | 0.55 (0.24) | <.001 |
| *Graft characteristics* | | | | |
| CVC graft on day 7, mean (SD), APU/mm Hg | 0.77 (0.53) | 0.94 (0.55) | 0.44 (0.29) | <.001 |
| Day 28 necrosis extent, median (range), % | 13.0 (0.0–84.0) | 9.0 (0.0–19.0) | 42.0 (22.0–84.0) | <.001 |

APU, arbitrary perfusion units; CVC, cutaneous vascular conductance.
Data are expressed as median (range) for nonnormally distributed continuous variables, mean (SD) for normally distributed continuous variables, or No. (%) for categorical variables. All skin grafts on the face and scalp were full-thickness grafts, whereas all grafts on the upper and lower limbs were split-thickness grafts.

*Univariable linear regression based on perfusion*

Table 2 shows the univariable linear regression models based on perfusion. The highest $R^2$ value, 0.75, was observed for graft bed perfusion, meaning that 75% of the variability in necrosis extent could be explained by this variable. Specifically, each unit increase in graft bed perfusion reduced necrosis extent by 41 percentage points. The predictive capacity for necrosis was lower on day 7, with an $R^2$ value of 0.46, and each unit increase in graft perfusion reduced necrosis extent by 21 percentage points. Because the 95%CIs for the linear regression $\beta$ coefficients did not overlap, the differences in the mean estimated effects were significant.

*Correlation analysis between other nonperfusion characteristics and necrosis*

Table 3 describes the correlations between patient, defect, and graft characteristics and necrosis extent. Only age ($r$ = −0.28), defect location on the face ($r$ = −0.29), and defect location on the lower limb ($r$ = 0.35) were significantly correlated with necrosis extent. None of

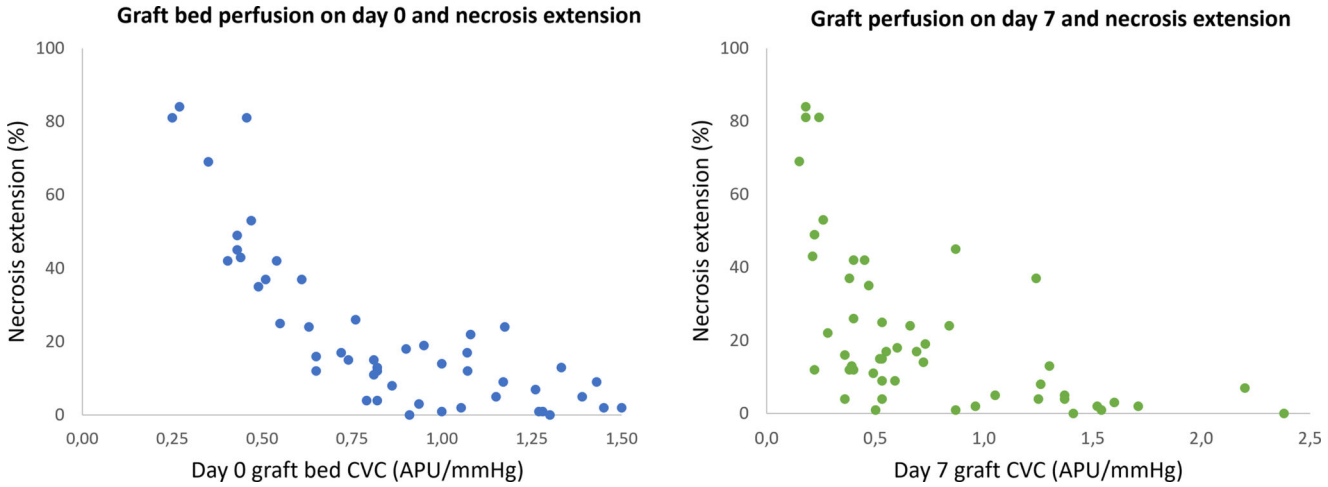


**Fig. 2.** Relationship between perfusion and necrosis extent. Scatterplots of perfusion, measured as cutaneous vascular conductance (CVC), in arbitrary perfusion units (APU)/mm Hg, on the graft bed intraoperatively and on the graft on day 7, and necrosis extent on day 28.

**Table 2**
Univariable linear regression models of necrosis extent based on perfusion of the defect bed on day 0 and the graft on day 7.

| Univariate model | *b* | *P* | $CI_{95\%}$ *b* | | Model summary |
|---|---|---|---|---|---|
| *Constant* | 0.12 | <0.001 | 0.09 | 0.16 | $R^2 = 0.75$ |
| Ln (CVC graft bed) | −0.41 | <0.001 | −0.47 | −0.34 | $F$ (1, 53) = 158.9 $P < 0.001$ |
| *Constant* | 0.10 | <0.001 | 0.05 | 0.16 | $R^2 = 0.46$ |
| Ln (CVC graft day 7) | −0.21 | <0.001 | −0.28 | −0.15 | $F$ (1, 53) = 46.8 $P < 0.001$ |

CVC, cutaneous vascular conductance; ln, natural logarithm.
$\beta$ coefficients represent the estimated change in necrosis extent for each 1-unit increase in ln(CVC).

these variables explained more than 11% of the variation in necrosis extent (Table 4).

*Multivariable linear regression analysis*

On day 0, adjustment of the model combining graft bed perfusion with age and defect location ($F = 41.0$; $P < .001$) was worse than that of the model with graft bed perfusion alone ($F = 158.9$; $P < .001$), despite the same $R^2$ value (Table 5). On day 0, the best predictive model for necrosis extent can be expressed as follows: necrosis extent = 0.12 – 0.41 × ln(CVC graft bed).

A similar finding was observed for graft perfusion on day 7, with the univariable model showing better adjustment ($F = 46.8$) than the multivariable model ($F = 13.0$) (Table 5). On day 7, necrosis extent can be predicted by graft perfusion according to the following formula: necrosis extent = 0.10 – 0.21 × ln(CVC graft day 7).

*Predictors of clinically significant necrosis*

Clinically significant necrosis, defined as necrosis extent of 20% or greater, developed in 18 of 55 grafts (32.7%); 12 of these grafts (66.7%) were located on the lower limb, and all were split-thickness grafts. Graft bed perfusion in the group with necrosis extent of 20% or greater was approximately half that measured in the group with necrosis extent less than 20% (0.55 vs 1.06 APU/mm Hg; $P < .001$).

Binary logistic regression models were created using graft bed perfusion alone or combined with lower limb location, which had been identified as an independent predictor of clinically significant necrosis. To prevent redundancy, graft type was not included in the regression model because all split-thickness grafts with necrosis extent of 20% or greater corresponded to lower limb grafts. Both models were statistically significant, but the accuracy of the univariable model (90.9%) was higher than that of the multivariable model (67.3%), indicating that perfusion alone was a better predictor than perfusion combined with lower limb location.

**Table 3**
Pearson correlation coefficients between participant, defect, and graft characteristics and necrosis extent on day 28.

| Characteristics | Correlation with necrosis extent, *r* | *P* value |
|---|---|---|
| *Participant characteristics* | | |
| Age | −0.28 | .04 |
| Sex | 0.003 | .98 |
| Arterial hypertension | 0.14 | .92 |
| Dyslipidemia | 0.05 | .77 |
| Diabetes mellitus | −0.17 | .22 |
| Current smoking | 0.24 | .08 |
| Antiplatelet therapy | −0.03 | .83 |
| Anticoagulant therapy | −0.11 | .44 |
| *Defect characteristics* | | |
| Scalp location | −0.05 | .73 |
| Face location | −0.29 | .03 |
| Upper limb location | −0.15 | .26 |
| Lower limb location | 0.35 | .01 |
| Defect area | −0.06 | .65 |
| *Graft characteristics* | | |
| Type of graft | −0.26 | .05 |

**Table 4**
Univariable linear regression models of necrosis extent based on age and anatomic location of the defect.

| Univariate model | *b* | *P* | $CI_{95\%}$ *b* | | Model summary |
|---|---|---|---|---|---|
| *Constant* | 0.81 | 0.01 | 0.22 | 1.39 | $R^2 = 0.06$ |
| Age | −0.01 | 0.04 | −0.02 | 0.00 | $F(1, 53) = 4.3$ |
| | | | | | $P = 0.04$ |
| *Constant* | 0.24 | < 0.001 | 0.18 | 0.30 | $R^2 = 0.10$ |
| Face | −0.18 | 0.03 | −0.32 | −0.04 | $F(1, 53) = 6.8$ |
| | | | | | $P = 0.01$ |
| *Constant* | 0.15 | < 0.001 | 0.08 | 0.22 | $R^2 = 0.11$ |
| Lower limb | 0.16 | 0.01 | 0.04 | 0.27 | $F(1, 53) = 7.6$ |
| | | | | | $P = 0.01$ |

$\beta$ coefficients represent the estimated change in necrosis extent associated with each predictor. Location variables were coded as binary variables.

**Table 5**
Multivariable linear regression models including graft bed perfusion on day 0 and graft perfusion on day 7.

| Multivariate model | *b* | *P* | $CI_{95\%}$ *b* | | Model summary |
|---|---|---|---|---|---|
| *Day 0* | | | | | |
| *Constant* | 0.13 | 0.40 | −0.19 | 0.46 | |
| Ln (CVC graft bed) | −0.40 | < 0.001 | −0.47 | −0.32 | $R^2 = 0.75$ |
| Age | −0.01 | 0.79 | −0.04 | 0.03 | $F(4, 50) = 41.0$ |
| Face | 0.30 | 0.47 | −0.05 | 0.11 | $P < 0.001$ |
| Lower limb | 0.06 | 0.06 | −0.04 | 0.13 | |
| *Day 7* | | | | | |
| *Constant* | 0.23 | 0.34 | −0.26 | 0.72 | |
| Ln (CVC graft day 7) | −0.20 | < 0.001 | −0.28 | −0.12 | $R^2 = 0.47$ |
| Age | −0.002 | 0.49 | −0.01 | 0.00 | $F(4, 50) = 13.0$ |
| Face | 0.04 | 0.55 | −0.09 | 0.17 | $P < 0.001$ |
| Lower limb | 0.1 | 0.04 | 0.00 | 0.19 | |

CVC, cutaneous vascular conductance; ln, natural logarithm.
$\beta$ coefficients represent the estimated change in necrosis extent associated with each predictor. Location variables were coded as binary variables.

For each 0.1 APU/mm Hg increase in graft bed CVC, the odds of clinically significant necrosis decreased by 57% (OR, 0.43; 95%CI, 0.28–0.68). This interpretation was based on rescaling CVC, initially ranging from 0.65 to 1.73 APU/mm Hg, by multiplying it by 10 to obtain a new range.

### *ROC curves for clinically significant necrosis*

ROC curves assessing the predictive capacity for necrosis extent of 20% or greater based on perfusion on days 0 and 7 are presented in Fig. 3. The area under the curve was 0.92 (95%CI, 0.83–1.00) on day 0 and 0.81 (95%CI, 0.69–0.94) on day 7. The best perfusion threshold values for necrosis extent of 20% or greater were 0.64 and 0.48 APU/mm Hg on days 0 and 7, respectively. The day 0 threshold showed the highest positive predictive value (100%) and negative predictive value (93%). On day 7, the positive predictive value was 68%, and the negative predictive value was 86%.

## Discussion

This study is the first to quantify the relationship between perfusion and graft necrosis. It highlights the role of graft bed perfusion in skin graft viability, which was by far more important than any other variable studied. Three-quarters of the variation in necrosis extent could be explained by graft bed perfusion alone. We also identified a graft bed perfusion threshold of 0.64 APU/mm Hg that accurately predicted the development of clinically significant graft necrosis. This finding may support decisions regarding immediate or delayed skin graft closure and may help determine the appropriate timing for grafting after nonimmediate closure. We also identified a graft perfusion threshold on day 7 of 0.48 APU/mm Hg that predicted necrosis extent of 20% or greater, with a negative predictive value of 86%. In clinical practice, this information could be used to identify patients with more favorable graft healing who may require less frequent wound care.

Skin graft necrosis may complicate 5–66% of these procedures, depending on the anatomic location and type of graft used, and often requires prolonged medical care, repeated wound dressings, debridement, or even regrafting.[1,16] Previous studies have shown the benefits of nonimmediate skin graft closure in allowing the development of well-perfused granulation tissue, thereby reducing the risk of necrosis. However, nonimmediate closure does not necessarily guarantee the absence of late graft necrosis.[18,19] The acquisition of pink coloration of the graft surface during the first week is frequently used as an inaccurate sign of probable survival.[20] Nevertheless, the decision to perform immediate or delayed skin grafting should be based on objective measurements of predictive factors for necrosis rather than on experiential knowledge alone.

Among the many noninvasive methods available for skin perfusion assessment in skin flaps, only a few, such as infrared thermal imaging, optical coherence tomography, laser Doppler imaging, and LSCI, have been used in skin grafts.[21–23] Infrared thermal imaging has a time lag between perfusion and temperature changes and lacks specificity for temperature-related variations.[10] Optical coherence tomography angiography has a penetration depth of 1.5 mm but a small field of view, approximately 9 mm × 9 mm, which limits the assessment of whole-graft revascularization.[21] Laser Doppler imaging has excellent spatial resolution but is slow because the laser scans across the skin and dwells briefly at each point.[24] We used LSCI because it overcomes the limitations of other techniques by offering rapid whole-graft perfusion measurements with excellent spatial and temporal resolution, making it suitable for

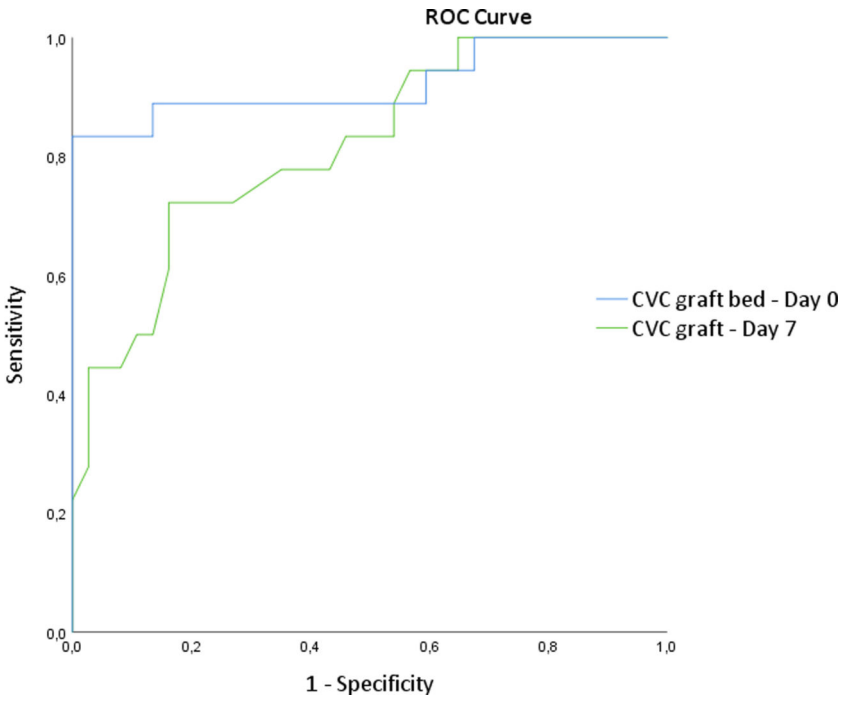


**Fig. 3.** ROC curves for clinically significant necrosis. Receiver operating characteristic (ROC) curves for clinically significant necrosis based on day 0 graft bed perfusion and day 7 graft perfusion. The area under the curve on days 0 and 7 was 0.92 and 0.81, respectively.

intraoperative and postoperative use while maintaining asepsis.[13] In addition to the previously known applications of LSCI in the management of burn wounds and chronic nonhealing wounds, particularly for identifying healing potential, this study introduces a new utility for LSCI in the treatment of surgical wounds with skin grafts in an oncologic setting.[25,26]

Despite its innovative nature, this study has several limitations. It could not account for other factors that might influence the outcome, including defect depth, degree of coaptation to the graft bed, and graft type or thickness. We consistently used split-thickness grafts for limb defects, which were usually nonexposed, and full-thickness grafts for scalp and facial defects, which were cosmetically sensitive. This precluded an exhaustive analysis based on graft type independent of anatomic location. However, split-thickness grafts are generally assumed to survive better than full-thickness grafts over poorly vascularized wound beds, although they are more prone to contraction and dyschromia, leading to poor cosmetic outcomes.[3]

Graft bed perfusion was evaluated after infiltration with lidocaine and epinephrine. Although this is standard practice in dermatologic surgery, epinephrine-induced vasoconstriction may temporarily decrease perfusion values and bias perfusion measurements. Nevertheless, we considered it appropriate to provide predictive models of graft necrosis in a real-life setting and therefore included epinephrine infiltration. Given the inclusion criteria, our results may apply only to skin cancer surgery.

Future studies should externally validate this evidence in new patient samples. A cost-effectiveness analysis would also be essential to assess the effect of systematic perfusion measurement with LSCI on costs related to graft necrosis.

## Conclusions

In skin graft surgery, the intra and postoperative perfusion analysis with LSCI can provide valuable information for necrosis prediction, bringing objective evidence to a field often guided by empiricism.

## Funding

The authors received funding from the European Academy of Dermatology and Venereology (EADV) to develop the project “Skin Grafts in Dermatologic Surgery: A Prospective Study of Vascularisation and Predictive Factors of Necrosis Using Laser Speckle Contrast Analysis” (project proposal PPRC-2023-0049).

## Conflicts of interest

None declared.

## Acknowledgment

The authors thank Dr Margarida Marques for her collaboration in the statistical analysis of this study.

## References

1. Santos X, Iglesias I. Necrotic complications after skin grafts. In: *Skin Necrosis.* Springer Vienna; 2015:201–206, http://dx.doi.org/10.1007/978-3-7091-1241-0_34.
2. Sun L, Patel AJ. Outcomes of split vs full-thickness skin grafts in scalp reconstruction in outpatient local anaesthetic theatre. *Scars Burn Heal.* 2021;7, http://dx.doi.org/10.1177/20595131211056542, 20595131211056542.
3. Adams DC, Ramsey ML. Grafts in dermatologic surgery: review and update on full- and split-thickness skin grafts, free cartilage grafts, and composite grafts. *Dermatol Surg.* 2005;31:1055–1067, http://dx.doi.org/10.1111/j.1524-4725.2005.31831.
4. Capla JM, Ceradini DJ, Tepper OM, et al. Skin graft vascularization involves precisely regulated regression and replacement of endothelial cells through both angiogenesis and vasculogenesis. *Plast Reconstr Surg.* 2006;117:836–844, http://dx.doi.org/10.1097/01.prs.0000201459.91559.7f.
5. Garcia N, Lau LDW, Lo CH, Cleland H, Akbarzadeh S. Understanding the mechanisms of spontaneous and skin-grafted wound repair: the path to engineered skin grafts. *J Wound Care.* 2023;32:55–62, http://dx.doi.org/10.12968/jowc.2023.32.1.55.
6. Brinca A, Pinho A, Vieira R. Laser speckle contrast imaging for assessment of human skin graft microcirculation. *J Eur Acad Dermatol Venereol.* 2020;34, http://dx.doi.org/10.1111/jdv.16408.
7. Brinca A, Pinho A, Vieira R. Searching for a mathematical model for blood perfusion of random pattern skin flaps: a clinical pilot study using in vivo laser speckle contrast imaging. *J Eur Acad Dermatol Venereol.* 2018;32, http://dx.doi.org/10.1111/jdv.14997.

8. Heeman W, Steenbergen W, van Dam GM, Boerma EC. Clinical applications of laser speckle contrast imaging: a review. *J Biomed Opt*. 2019;24, http://dx.doi.org/10.1117/1.JBO.24.8.080901, 080901.
9. Carvalho Brinca AM, de Castro Pinho A, Costa Vieira RJD. Blood perfusion of random skin flaps in humans – in vivo assessment by laser speckle contrast imaging. *Dermatol Surg*. 2021;47:1421–1426, http://dx.doi.org/10.1097/DSS.0000000000003164.
10. Berggren J, Castelo N, Tenland K, et al. Reperfusion of free full-thickness skin grafts in periocular reconstructive surgery monitored using laser speckle contrast imaging. *Ophthalmic Plast Reconstr Surg*. 2021;37:324–328, http://dx.doi.org/10.1097/IOP.0000000000001851.
11. Russo-de la Torre F, Vieira R, Iglesias-Zamora ME. Estudio in vivo del flujo vascular del colgajo centollo mediante láser de contraste de imagen por puntos. *Actas Dermosifiliogr*. 2024;115:91–93, http://dx.doi.org/10.1016/j.ad.2023.03.007.
12. Linkous C, Pagan AD, Shope C, et al. Applications of laser speckle contrast imaging technology in dermatology. *JID Innov*. 2023;3:100187, http://dx.doi.org/10.1016/j.xjidi.2023.100187.
13. Mahé G, Rousseau P, Durand S, Bricq S, Leftheriotis G, Abraham P. Laser speckle contrast imaging accurately measures blood flow over moving skin surfaces. *Microvasc Res*. 2011;81:183–188, http://dx.doi.org/10.1016/j.mvr.2010.11.013.
14. Mahé G, Humeau-Heurtier A, Durand S, Leftheriotis G, Abraham P. Assessment of skin microvascular function and dysfunction with laser speckle contrast imaging. *Circ Cardiovasc Imaging*. 2012;5:155–163, http://dx.doi.org/10.1161/CIRCIMAGING.111.970418.
15. Henderson NJ, Fancourt M, Gilkison W, Kyle S, Mosquera D. Skin grafts: a rural general surgical perspective. *ANZ J Surg*. 2009;79:362–366, http://dx.doi.org/10.1111/j.1445-2197.2009.04890.x.
16. Stankiewicz M, Coyer F, Webster J, Osborne S. Incidence and predictors of lower limb split-skin graft failure and primary closure dehiscence in day-case surgical patients. *Dermatol Surg*. 2015;41:775–783, http://dx.doi.org/10.1097/DSS.0000000000000391.
17. Joyce W, White DW, Raven PB, Wang T. Weighing the evidence for using vascular conductance, not resistance, in comparative cardiovascular physiology. *J Exp Biol*. 2019;222, http://dx.doi.org/10.1242/jeb.197426, jeb197426.
18. Robinson JK, Dillig G. The advantages of delayed nasal full-thickness skin grafting after Mohs micrographic surgery. *Dermatol Surg*. 2002;28:845–851, http://dx.doi.org/10.1046/j.1524-4725.2002.02031.x.
19. David AP, Miller MQ, Park SS, Christophel JJ. Comparison of outcomes of early vs delayed graft reconstruction of Mohs micrographic surgery defects. *JAMA Facial Plast Surg*. 2019;21:89–94, http://dx.doi.org/10.1001/jamafacial.2018.1204.
20. Thornton J, Gosman A. Skin grafts, skin substitutes, and principles of flaps. *Sel Read Plast Surg*. 2004;10:1–78.
21. Deegan AJ, Lu J, Sharma R, Mandell SP, Wang RK. Imaging human skin autograft integration with optical coherence tomography. *Quant Imaging Med Surg*. 2021;11:784–796, http://dx.doi.org/10.21037/QIMS-20-750.
22. Klama-Baryła A, Kitala D, Łabuś W, Kraut M, Szapski M, Smętek W. Infrared thermal imaging as a method of improving skin graft qualification procedure and skin graft survivability. *Transplant Proc*. 2020;52:2223–2230, http://dx.doi.org/10.1016/j.transproceed.2020.01.108.
23. Wang J, Hao H, Huang H, Chen D, Han Y, Han W. The effect of adipose-derived stem cells on full-thickness skin grafts. *Biomed Res Int*. 2016;2016, http://dx.doi.org/10.1155/2016/1464725, 1464725.
24. Cracowski JL, Roustit M. Current methods to assess human cutaneous blood flow: an updated focus on laser-based techniques. *Microcirculation*. 2016;23:337–344, http://dx.doi.org/10.1111/micc.12257.
25. Zheng KJ, Middelkoop E, Stoop M, van Zuijlen PPM, Pijpe A. Validity of laser speckle contrast imaging for the prediction of burn wound healing potential. *Burns*. 2022;48:319–327, http://dx.doi.org/10.1016/j.burns.2021.04.028.
26. Dijkstra A, Guven G, van Baar ME, et al. Laser speckle contrast imaging, an alternative to laser doppler imaging in clinical practice of burn wound care: derivation of a color code. *Burns*. 2023;49:1907–1915, http://dx.doi.org/10.1016/j.burns.2023.04.009.